Induced Deactivation of Genes Encoding Chlorophyll Biosynthesis Enzymes Disentangles Tetrapyrrole-Mediated Retrograde Signaling

Hagen Schlicke[a], Annabel Salinas Hartwig[a], Vivien Firtzlaff[a], Andreas S. Richter[a], Christine Glässer[b], Klaus Maier[b], Iris Finkemeier[c] and **Bernhard Grimm[a,1]**

a Institute of Biology/Plant Physiology, Humboldt University Berlin, Philippstr. 13, Building 12, D 10115 Berlin, Germany
b Helmholtz Zentrum München, Deutsches Forschungszentrum für Gesundheit und Umwelt (GmbH), Ingolstädter Landstr. 1, 85764 Neuherberg, Germany
c Max-Planck-Institute for Plant Breeding Research, Plant Proteomics and Mass Spectrometry Group, Carl-von-Linné Weg 10, 50829 Cologne, Germany

ABSTRACT **In photosynthetic organisms, tetrapyrrole-mediated retrograde signals are proposed to contribute to a balanced nuclear gene expression (NGE) in response to metabolic activity in chloroplasts. We followed an experimental short-term approach that allowed the assessment of modified NGE during the first hours of specifically modified enzymatic steps of the Mg branch of tetrapyrrole biosynthesis, when pleiotropic effects of other signals can be avoided. In response to 24-h-induced silencing of *CHLH*, *CHLM*, and *CHL27* encoding the CHLH subunit of Mg chelatase, the Mg protoporphyrin methyltransferase and Mg protoporphyrin monomethylester cyclase, respectively, deactivated gene expression rapidly led to reduced activity of the corresponding enzymes and altered Mg porphyrin levels. But NGE was not substantially altered. When these three genes were continuously inactivated for up to 4 d, changes of transcript levels of nuclear genes were determined. *CHL27* silencing for more than 24 h results in necrotic leaf lesions and modulated transcript levels of oxidative stress-responsive and photosynthesis-associated nuclear genes (PhANGs). The prolonged deactivation of *CHLH* and *CHLM* results in slightly elevated transcript levels of PhANGs and tetrapyrrole-associated genes. These time-resolved studies indicate a complex scenario for the contribution of tetrapyrrole biosynthesis on NGE mediated by $^1O_2$-induced signaling and feedback-regulated ALA synthesis.**

Key words: plastid signal; transcription analysis; retrograde signal; tetrapyrrole metabolism; Mg protoporphyrin.

Schlicke H., Hartwig S., Firtzlaff V., Richter A., Glässer C., Maier K., Finkemeier I., and Grimm B. (2014). Induced deactivation of genes encoding chlorophyll biosynthesis enzymes disentangles tetrapyrrole-mediated retrograde signaling. Mol. Plant. **7**, 1211–1227.

INTRODUCTION

The genetic heterogeneity of photosynthetic organisms is explained by the origin of intracellular organelles, plastid, and mitochondrion. Based on the endosymbiotic theory, engulfed microorganisms evolved to the specific organelles, which play crucial roles in energy conversion (Martin et al., 2002). The genetic and metabolic activities in these organelles require proteins, which are synthesized in a tightly coordinated expression of nuclear and plastid genes. The proteome of *Arabidopsis thaliana* plastids consists of approximately 3000 proteins and its majority is encoded by nuclear genes. Only a few plastid-localized genes encode proteins which complete the complexes for photosynthesis, organellar gene expression, and protein synthesis (Abdallah et al., 2000; Leister, 2005; Joyard et al., 2009). Functional organelles require mutual exchange of information between the nucleus and the organelles by anterograde and retrograde signaling, respectively. The nuclear gene expression (NGE) administers functionality of

[1] To whom correspondence should be addressed. E-mail bernhard.grimm@rz.hu-berlin.de, tel. +49-30-2093-6119, fax +49-030-2093-6337.
© The Author 2014. Published by the Molecular Plant Shanghai Editorial Office in association with Oxford University Press on behalf of CSPB and IPPE, SIBS, CAS.
doi:10.1093/mp/ssu034, Advance Access publication 21 March 2014
Received 1 February 2014; accepted 18 March 2014

plastids and mitochondria by anterograde control. Thereby, the anterograde control coordinates not only the synthesis of nuclear-encoded proteins, but also their import into the organelles (Rodermel, 2001; Nott et al., 2006; Pesaresi et al., 2007; Pogson et al., 2008; Chi et al., 2013).

Retrograde signals emitted by components capable of sensing and communicating the developmental stage and the metabolic activities in chloroplasts and mitochondria (Rodermel, 2001). First experimental evidence for retrograde control of NGE indicated that photooxidative stress factors originating in the chloroplast transmit information to the nucleus to modulate NGE in response to the physiological state of plastids (Oelmuller and Mohr, 1986). Today it is known that multiple signals derived from various sources within the chloroplasts modulate NGE as a prerequisite for organelle development as well as for the adaption to several stresses and environmental changes. In the last decade, a multitude of reviews summarized the increasing number of published data, inter alia (Pogson et al., 2008; Woodson and Chory, 2012; Chi et al., 2013). The signals were grouped according to their emergence: (1) reactive oxygen species (ROS) and dedicated processes (Galvez-Valdivieso and Mullineaux, 2010; Kim and Apel, 2013), (2) organellar redox state (Baier and Dietz, 2005; Brautigam et al., 2009), (3) plastid protein synthesis (Gray et al., 2003; Pfannschmidt et al., 2009; Voigt et al., 2010), (4) tetrapyrrole intermediates (Mochizuki et al., 2008; Moulin et al., 2008; von Gromoff et al., 2008; Woodson et al., 2011; Terry and Smith, 2013), and (5) metabolites, like 3-phosphoadenosine 5′-phosphate (PAP) (Estavillo et al., 2011), methylerythritol cyclodiphosphate (MEcPP) (Xiao et al., 2012) and β-cyclocitral β-CC (Ramel et al., 2012).

The concept of plastid-derived retrograde signaling can be classified into two categories: the biogenic control and the operational control (Pogson et al., 2008). The biogenic control includes the bidirectional communication for the biogenesis of organelles at early developmental stages of seedlings. The operational control adjusts the organellar functions to the environmental changes by means of transducing signals from the plastids and modifying NGE. This concept implies that anterograde and retrograde signals are continuously required to enable optimal activity of plastids (and mitochondria) and to balance metabolic variations under normal and adverse environmental conditions. It is obvious that each plastid-derived signal is modulated by interaction with components of other signaling pathways (Estavillo et al., 2012; Chi et al., 2013). Hence, the optimized organellar function is a result of a combination and convergence of multiple signals.

Tetrapyrrole-mediated signaling has been proposed from the beginning of studies on retrograde signals (Susek et al., 1993; Kropat et al., 2000; Nott et al., 2006; Mochizuki et al., 2010; Terry and Smith, 2013). The tetrapyrrole biosynthetic pathway delivers essential but also highly photoreactive end-products, which are capable of light absorption, but also prone to oxidants, such as molecular oxygen. Therefore, the metabolic pathway is subject to an intricate control system, including multiple feedback cues. Modulation of the rate-limiting step of 5-aminolevulinic acid (ALA) synthesis, the initial steps of the chlorophyll-synthesizing Mg branch, and heme metabolism have been demonstrated to elicit a plastid-to-nucleus signaling for the coordination of NGE, in response to the physiological state of plastid-localized tetrapyrrole biosynthesis (Mochizuki et al., 2001; Larkin et al., 2003; Strand et al., 2003; Woodson et al., 2011; Czarnecki et al., 2012). In this context, the metabolite magnesium protoporphyrin (MgP) was suggested to act as a signal or secondary messenger molecule, once it is released from plastids. This hypothesis was tested by several research papers and questioned in reviews (Mochizuki et al., 2008; Moulin et al., 2008; Mochizuki et al., 2010), because a correlation could not be demonstrated between steady-state levels of MgP and modulation of *LHCB* expression encoding light-harvesting chlorophyll-binding protein of photosystem II (LHCB) (Mochizuki et al., 2010), or any other photosynthesis-associated nuclear gene (PhANG) (Ruckle et al., 2007). Therefore, it remains open whether a potentially phototoxic compound could be a good candidate for a plastid-to-nucleus signaling molecule.

We aimed to specify and separate individual signals and asked whether tetrapyrrole biosynthesis releases plastid-derived signals that affect NGE. To assay tetrapyrrole-mediated retrograde signaling, it was necessary to induce modulation in metabolic activities of the pathway without a significant effect of physiological downstream processes. Thus, for the elucidation of a specific and unique tetrapyrrole signal for adjusting NGE, pleiotropic effects were avoided by ensuring intact and entire functional chloroplasts. This concept excludes the use of constitutive mutants, which are affected by mutation from the early embryogenesis, as well as the application of herbicides during germination as manipulators of plastid function, such as norflurazon. Instead, an inducible conditional gene deactivation of green adult plants was used to demonstrate an operational signaling from chloroplasts.

In this report, we focus on the assessment of potential retrograde signals derived from the tetrapyrrole biosynthesis pathway, particularly on magnesium porphyrins. Chemically induced short-term inactivation of genes involved in three successive enzymatic steps of chlorophyll biosynthesis, namely the insertion of Mg^{2+} into protoporphyrin (PIX) catalyzed by Mg chelatase, methyl esterification of MgP by MgP methyltransferase (CHLM), and the subsequent formation of an isocyclic ring from the 13-methyl propionate of magnesium protoporphyrin monomethylester (MgPME) by MgPME oxidative cyclase, were used to evaluate changes in NGE. Prior to the global

transcript analyses of wild-type and short-term modulated transgenic plants, we confirmed that only the targeted enzymatic step of each transgenic line used in the studies was inactivated. In a proof of concept, we aimed to analyze to which extent initial modulations of tetrapyrrole biosynthesis releases signals for modulation of the transcriptome in green *Arabidopsis* seedlings.

RESULTS

Short-Term Gene Silencing Causes Rapid Reduction of Transcript Levels and Altered Enzyme Activities within 24 h

Transgenic *Arabidopsis* lines were generated carrying inducible RNAi transgene constructs for deactivation of the *CHLH* gene encoding the CHLH subunit of Mg chelatase, the *CHLM* gene encoding MgP methyltransferase, and the *CHL27* gene encoding the CHL27 subunit of MgPME cyclase. A single representative line was selected from the three sets of transgenic lines carrying the inducible gene inactivation construct for the respective target gene. This line is characterized by rapid gene deactivation following dexamethasone induction. The inducible gene deactivation was functional in the offspring of multiple generations within 3 y of the research period. The inactivation of each enzymatic step was compared to dexamethasone-treated wild-type. Gene deactivation in 10-day-old seedlings reduced the mRNA content of *CHLH*, *CHLM*, and *CHL27* by more than 90% within 24 h after RNAi induction (Figure 1A). Following the described short-term silencing, the seedlings did not display macroscopic phenotypes when compared to wild-type (Figure 1B).

Since the investigated RNAi lines phenotypically resembled wild-type seedlings 24 h after induced RNAi silencing, we first investigated changes in the metabolic pathway of chlorophyll biosynthesis. Decreased *CHLH*, *CHLM*, and *CHL27* transcript levels resulted in a substantial reduction of activity of Mg chelatase, MgP methyltransferase, or MgPME cyclase, respectively, in comparison to dexamethasone-treated wild-type seedlings (Figure 1C–1E). Because the short-term gene deactivation substantially lowered the activity of the targeted enzymes, the steady-state levels of tetrapyrrole intermediates were examined in seedlings after 24 h of induced RNAi silencing.

Although Mg chelatase activity decreased (Figure 1C), it is remarkable that PIX, the substrate of Mg chelatase, did not accumulate in CHLH RNAi seedlings (Figure 2A) in comparison to wild-type, but magnesium porphyrins were not detectable (Figure 2B and 2C). Lowered cyclase activity in CHL27 RNAi plants (Figure 1E) resulted in a massive accumulation of MgPME (Figure 2C), which is the substrate of the MgPME cyclase. Increased MgP steady-state levels (Figure 2B) were also determined and most likely resulted from the tailback of porphyrin intermediates. Despite the reduced MgP methyltransferase activity (Figure 1D), the CHLM RNAi line showed only a slight increase of porphyrin steady-state levels (Figure 2A–2C) 24 h after induced RNAi gene silencing. The reduced enzyme activities and altered Mg porphyrin steady-state levels in all three RNAi lines did not cause any changes in the chlorophyll contents compared to wild-type seedlings after 24-h perturbation of the metabolic pathway (Figure 2D). Interestingly, the ALA synthesis capacity was reduced in seedlings of the CHLH RNAi and CHLM RNAi lines (Figure 2E). This observation agrees with the results previously obtained from *CHLH* and *CHLM* antisense tobacco lines (Papenbrock et al., 2000; Alawady and Grimm, 2005). The decreased ALA synthesizing capacity after 24 h of RNAi silencing is proposed to be a consequence of the regulatory feedback, after deactivation of enzymes in the Mg branch (Cornah et al., 2003; Czarnecki and Grimm, 2012). The moderate increase of ALA synthesis capacity in the CHL27 RNAi line (Figure 2E) resembles the elevated ALA synthesis observed in *LCAA* antisense tobacco lines, which showed reduced expression of this additional subunit of MgPME cyclase (Albus et al., 2012).

Modified Porphyrin Levels Do Not Affect the Expression of PhANGs and Tetrapyrrole-Associated Genes

Although the short-term metabolic inactivation of gene expression caused reduced enzyme activities and modified Mg porphyrin levels, no macroscopic changes were detectable in the plants, including no changes in chlorophyll content (Figure 2D). A transcriptome analysis of the three RNAi lines was performed 24 h after induction of RNAi gene silencing to investigate the effect of altered porphyrin steady-state levels on NGE. Ten-day-old seedlings were harvested from two different cultivations. The transcript profiling revealed 206, 188, and 206 differentially expressed genes in seedlings of the CHLH RNAi, CHLM RNAi, and CHL27 RNAi line, respectively (Supplemental Table 1), with transcript levels deviating at least two-fold compared to dexamethasone-treated wild-type. Among the genes with altered transcript levels (Supplemental Table 1), no PhANGs, tetrapyrrole synthesis-associated genes, or genes encoding components associated with any obvious chloroplast function were found. It is also important to emphasize that ROS marker genes proposed by Galvez-Valdivieso and Mullineaux (2010) are not distinctively up-regulated. Changes in expression of these genes have been previously associated with deregulation of tetrapyrrole biosynthesis and increasing photosensitization by accumulating porphyrins (Apel and Hirt, 2004; Kim et al., 2008).

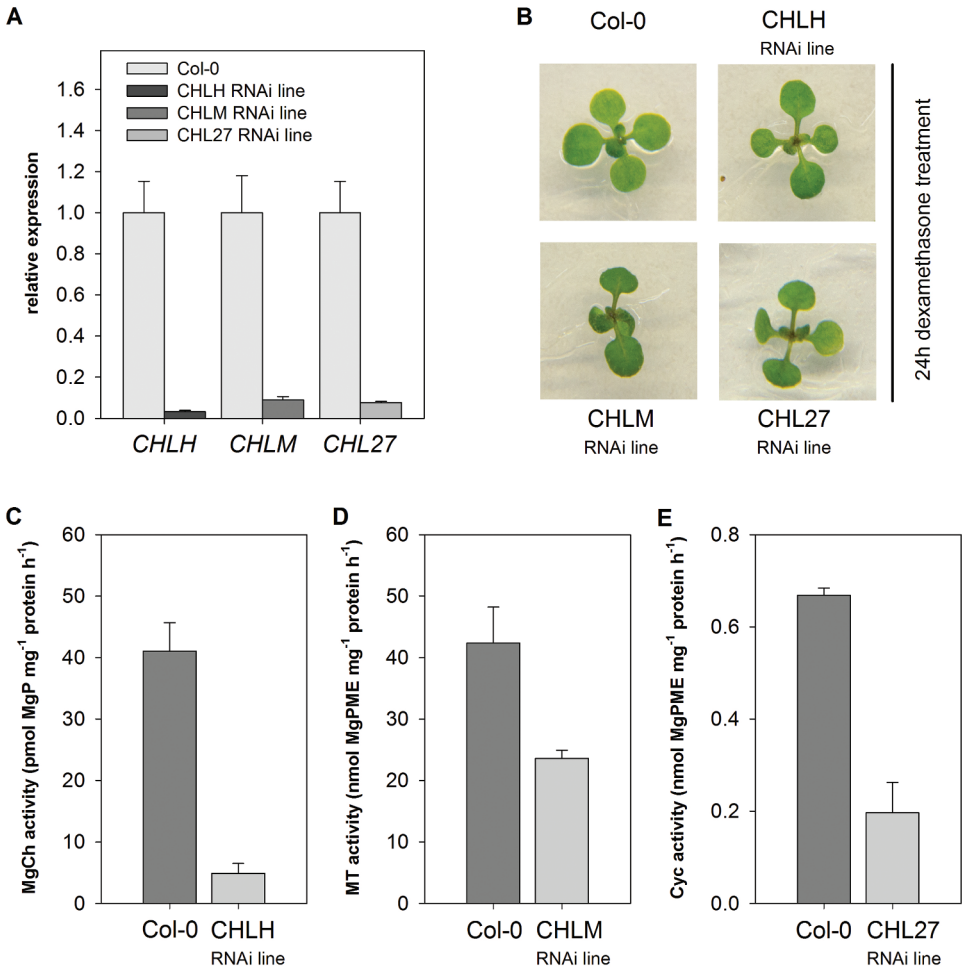

Figure 1 Genetic and Biochemical Analysis of Transgenic Lines after 24-h Gene Silencing of *CHLH*, *CHLM*, and *CHL27*, Respectively.

(A) Transcript analysis of 10-day-old seedlings of the CHLH, CHLM, and CHL27 RNAi lines growing on MS in continuous light 24 h after induced gene silencing. Transcript levels were calculated as relative expression ($2^{-\Delta\Delta CT}$) according to Livak and Schmittgen (2001) in comparison to dexamethasone-treated wild-type plants as control and *Actin2* as a reference gene. The *CHLH*, *CHLM*, and *CHL27* transcript contents were decreased in the corresponding RNAi lines to less than 10% of the wild-type content. Data are given as means and SD of three biological replicates.

(B) Phenotypes of 14-day-old *Arabidopsis* wild-type and RNAi lines. Seedlings grew in continuous light of 100 μmol photon m^{-2} s^{-1} treated for 24 h with dexamethasone.

(C–E) Enzyme activity assays with crude *Arabidopsis* chloroplast extracts 24 h after induction of RNAi silencing for (C) Mg chelatase (MgCh), (D) MgP methyltransferase (MT), and (E) MgPME cyclase (Cyc) given as metabolic rate of the substrate. Data are given as means and SD of three biological replicates. All experiments were repeated at least twice.

Transcriptome Analysis Reveals a Set of Commonly Deregulated Genes as a Side Effect of the Vector System

The evaluation of microarray data shows a group of 133 commonly deregulated genes after 24-h deactivation of *CHLH*, *CHLM*, and *CHL27* (Supplemental Table 2). However, an additional transcriptome analysis of a control RNAi line containing a pOpOff2(km):LUC gene construct that deactivates the *LUC* gene encoding firefly luciferase (Huang et al., 2011) was performed to prove whether the deregulation of NGE in the three lines is exclusively the result of disrupted tetrapyrrole biosynthesis (Figure 3). This analysis presented in the Venn diagram revealed that 99 of the 133 genes were consistently either up- or down-regulated in the LUC RNAi line (Figure 3A and Supplemental Table 2), indicating an integrative source of signals which leads to

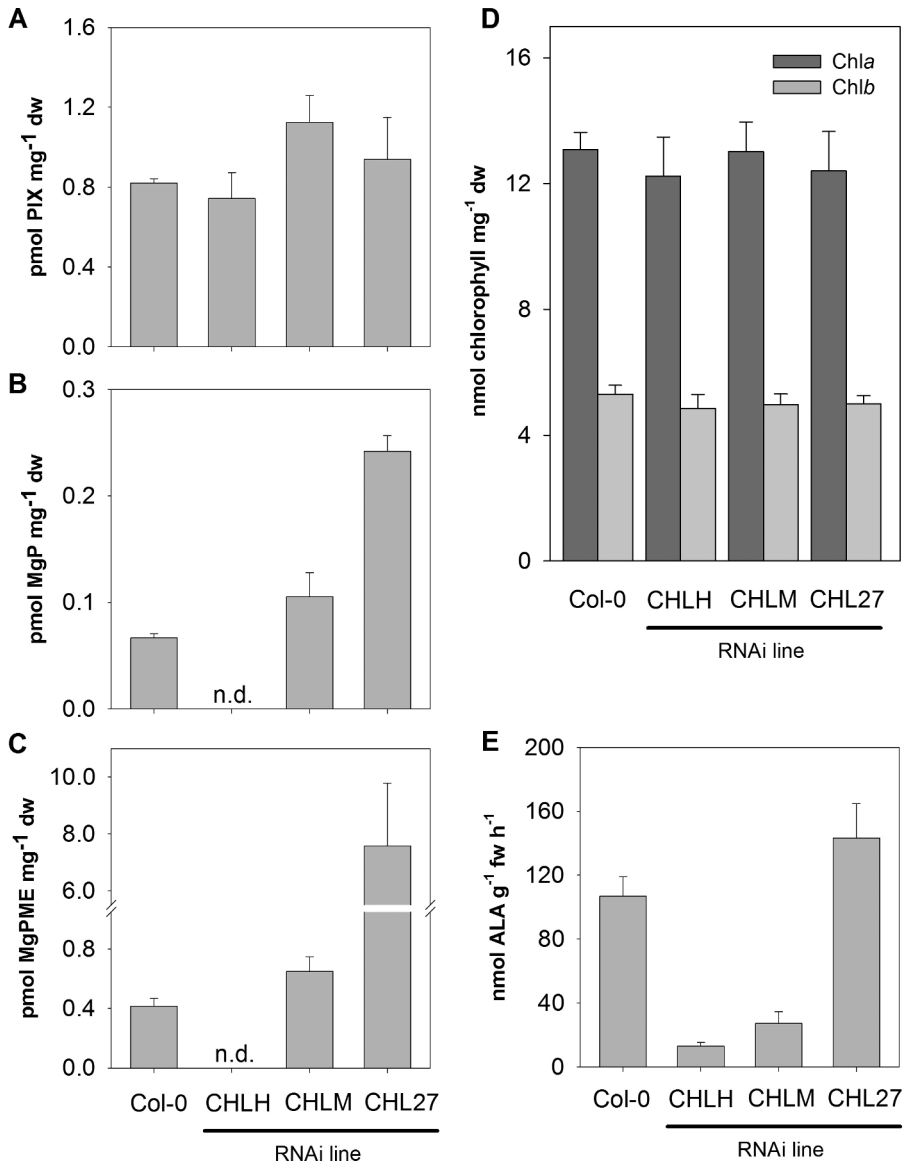

Figure 2 Chlorophyll Content and Steady-State Levels of Tetrapyrrole Biosynthesis Intermediates 24 h after *CHLH*, *CHLM*, and *CHL27* Gene Silencing.

(A–C) Steady-state levels of porphyrins 24 h after treatment with dexamethasone and induced RNAi gene silencing: (A) protoporphyrin IX (PIX), (B) magnesium protoporphyrin (MgP), (C) MgP monomethylester (MgPME).

(D) The chlorophyll content of seedlings of the three RNAi lines and wild-type determined 24 h after induced gene silencing.

(E) Analysis of the ALA synthesizing capacity in transgenic lines in comparison to wild-type after 24 h of induced *CHLH*, *CHLM*, and *CHL27* gene silencing. Plants were grown on soil for 14 d under 100 µmol photon m^{-2} s^{-1} light intensity.

an altered NGE. Modified transcript levels of several genes analyzed in the microarray were confirmed by quantitative reverse transcriptase polymerase chain reaction (qRT–PCR) (Supplemental Table 3). This indicates the quality and robustness of the transcriptomic data obtained by microarray analysis. Moreover, comparative qRT–PCR analysis of dexamethasone-treated RNAi line and untreated-RNAi line revealed that the constitutive expression of the chimeric transcription factor encoded on the pOpOff2 vector did not yield altered mRNA amounts of investigated genes (data not shown). Thus, the analysis disclosed an unspecific effect on NGE triggered by the RNAi system possibly due to overexpression of small interference RNA (siRNA). The option that the chimeric transcription factor promotes also the expression of *Arabidopsis* endogenes after dexamethasone treatment needs to be further investigated.

The genes which were deregulated in at least one of the three RNAi lines and additionally in the LUC RNAi line

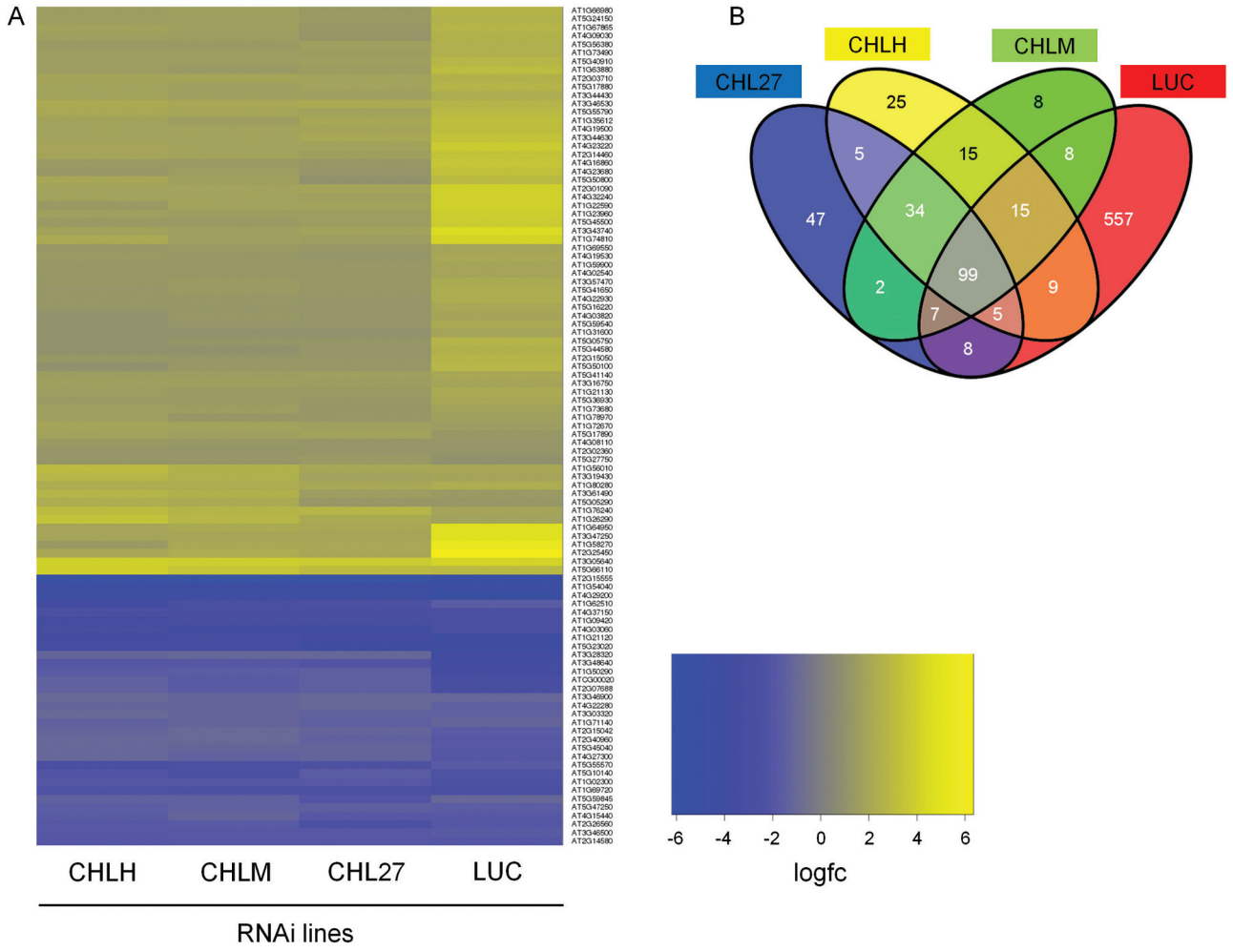

Figure 3 Comparative Microarray Analysis of CHLH, CHLM, CHL27, and LUC RNAi Lines 24 h after RNAi Induction.

(A) Heat map analysis of commonly deregulated genes 24 h after induction of RNAi in the four RNAi lines. The LUC RNAi line contains a part of the firefly luciferase gene sequence which did not interfere with *Arabidopsis thaliana* transcripts after activation of the RNAi machinery. Genes showing a two-fold increase or decrease of the fold change (FC) compared to wild-type and a *p*-value of less than 0.05 in all four RNAi lines are depicted. Almost all these genes are uniformly deregulated.

(B) The Venn diagram shows the central cluster of 99 commonly deregulated genes 24 h after dexamethasone activation of the RNAi mechanism. The intersections represent the number of mutually deregulated genes in the corresponding RNAi lines. Supplemental Table 2 contains the lists of genes representing the intersections.

show a similar deregulation (data not shown; Figure 3B). The clusters without intersections to the LUC RNAi line contain the genes which were potentially deregulated as a result of impaired tetrapyrrole biosynthesis (Figure 3B and Supplemental Table 4). Cluster 1 (Supplemental Table 4) includes all 34 genes which were commonly deregulated in the three RNAi lines for tetrapyrrole enzymes. A high number of these genes is also deregulated in the LUC RNAi line but do not conform to the significance criteria. Clusters 5–7 (Supplemental Table 4) contain commonly deregulated genes in two RNAi lines each, while clusters 2–4 comprise genes deregulated exclusively in one of the three RNAi lines for chlorophyll synthesis. It is worth mentioning that the CHLM RNAi and CHLH RNAi lines share more common deregulated genes than any other twin combination, while the most exclusively deregulated genes are found in the CHL27 RNAi line after 24 h of significant inactivation of the cyclase activity. When all genes are assigned to GO categories, no significant over-representation of genes for specific categories could be derived using the ***G**ene **O**ntology en**RI**chment anaLysis* and *visuaLizAtion tool* (Eden et al., 2009) and the deregulated genes of the LUC RNAi line as background set. Only the 99 commonly deregulated genes show an enrichment of the GO category defense response.

Using the software Genevestigator (Hruz et al., 2008), expression profiles of all the deregulated genes upon gene

silencing of chlorophyll synthesis genes (clusters 1–7) were selected from publicly available comparative transcriptomic analyses of retrograde signaling mutants (*gun1*, *gun5*) with and without norflurazon treatment in comparison to wild-type controls. The tables in Supplemental Figure 1 indicate the variation of expression of these genes and allow comparison and potential assignment of these genes to typical PhANGs, which are characterized by a commonly accepted modulated expression pattern in *gun* mutants compared to wild-type under adverse conditions, like norflurazon treatment. Among the analyzed 131 genes, only eight genes were found showing a derepression of expression in the *gun* mutants compared to wild-type after norflurazon treatment (Supplemental Figure 1). Further *in silico* analysis could not reveal any direct functional correlation between these genes and plastid function.

In summary, by means of the transcriptome analysis, we could not assign specific sets of deregulated genes or single genes to functions in the plastid–nucleus communication and we conclude that 24 h of *CHLH*, *CHLM*, and *CHL27* silencing did not likely address genes with certain significance in retrograde signaling.

Four-Day Deactivation of Chlorophyll Biosynthesis Genes Causes Drastic Phenotypical Changes

In continuation, the questions emerged how the RNAi lines adapted to the long-term silencing of *CHLH*, *CHLM*, and *CHL27*, and how the long-lasting deactivation of these genes affects NGE. For a 4-d RNAi inactivation, the seedlings were grown on MS medium to ensure a constant supply of dexamethasone. For better differentiation between 24-h- and 96-h-induced RNAi silencing, we refer to short-term and long-term gene silencing. We harvested seedlings after 1, 2, and 4 d of induced gene silencing. The transcript levels of the target genes *CHLH*, *CHLM*, and *CHL27* remained low or decreased further (Figure 4G–4I), indicating a continuously specific inhibition of the respective enzymatic step during the experimental procedure. Due to the inhibition of Mg chelatase reaction in the CHLH RNAi line, the downstream intermediates, such as MgP, MgPME, and Pchlide, showed decreasing steady-state levels during the induction period, whereas PIX content increased approximately three-fold after a 4-d repression of the *CHLH* expression (Figure 5A). PIX did not drastically accumulate in comparison to wild-type and, hence, did not cause leaf necrosis, as can be observed after inhibition by herbicides or declined content of protoporphyrinogen oxidase 1 and ferrochelatase 2, respectively (Papenbrock and Grimm, 2001; Lermontova and Grimm, 2006). However, as a consequence of a reduced chlorophyll biosynthesis after 4 d of *CHLH* silencing, the newly developed leaves showed reduced green pigmentation (Figures 5D and Figure 6A) and an elevated chlorophyll a/b ratio in comparison to wild-type and the other transgenic seedlings (Figure 6B).

The reduced MgP methyltransferase activity did not result in strong changes of intermediate steady-state levels (Figure 5B). It is important to note that not even MgP, the substrate of CHLM, accumulated as a result of *CHLM* silencing. The CHLM RNAi line grew phenotypically similar to wild-type (Figure 5D) within the 4 d of continuously induced *CHLM* deactivation. In contrast, the limited MgPME cyclase activity in dexamethasone-treated CHL27 RNAi seedlings resulted in a continuous increase of its substrate, MgPME (Figure 5C), to phototoxic concentrations and also in the weaker accumulation of the upstream intermediate MgP. The relative values of PIX and Mg porphyrins during the 4-d gene silencing are depicted in Supplemental Table 5. Hence, necrotic leaf lesions (Figure 5D) and, consequently, reduced chlorophyll contents (Figure 6A) emerged after 4 d of *CHL27* silencing.

The ALA synthesis rate declined in the CHLH RNAi line already after 24 h of *CHLH* deactivation, while the CHLM RNAi line displayed only a slight reduction in ALA synthesis capacity within the 4-d period. The ALA synthesis of the CHL27 RNAi line dropped after 2 d of gene silencing, and correlates with a photooxidative inactivation of pigment synthesis and the formation of leaf necrosis (Figure 6D). The heme content was measured during the induced long-term gene silencing and no change was observed in all plants at any time of analysis with the exception of a reduced level (70% relative to wild-type) in the CHL27 RNAi line after 4 d (Figure 6D).

PhANGs Show Altered Expression in the RNAi Lines during Long-Term Gene Silencing

To monitor the impact of cumulative defects in plastid functions on NGE resulting from impaired chlorophyll biosynthesis, we investigated the kinetics of transcript accumulation of selected PhANGs, ROS marker genes, and tetrapyrrole biosynthesis-associated genes within a 4-d period of induced *CHLH*, *CHLM*, and *CHL27* gene silencing in comparison to time point zero (t_0). Keeping in mind that the PhANG transcript levels did not significantly change in the first 24 h after induced RNAi gene silencing, a normal PhANG expression correlates with normal plastid integrity (Terry and Smith, 2013). But the long-term deactivation of genes associated with early enzymatic steps of chlorophyll biosynthesis led to a differentiated pattern of modified transcript levels of selected PhANG representatives. The mRNA contents of *RBCS*, *LHCB1.2*, and *PC* encoding the small subunit of ribulose-1,5-bisphosphate carboxylase, LHCB of photosystem II, and plastocyanin, respectively, were moderately elevated in the CHLH RNAi and CHLM RNAi lines over the

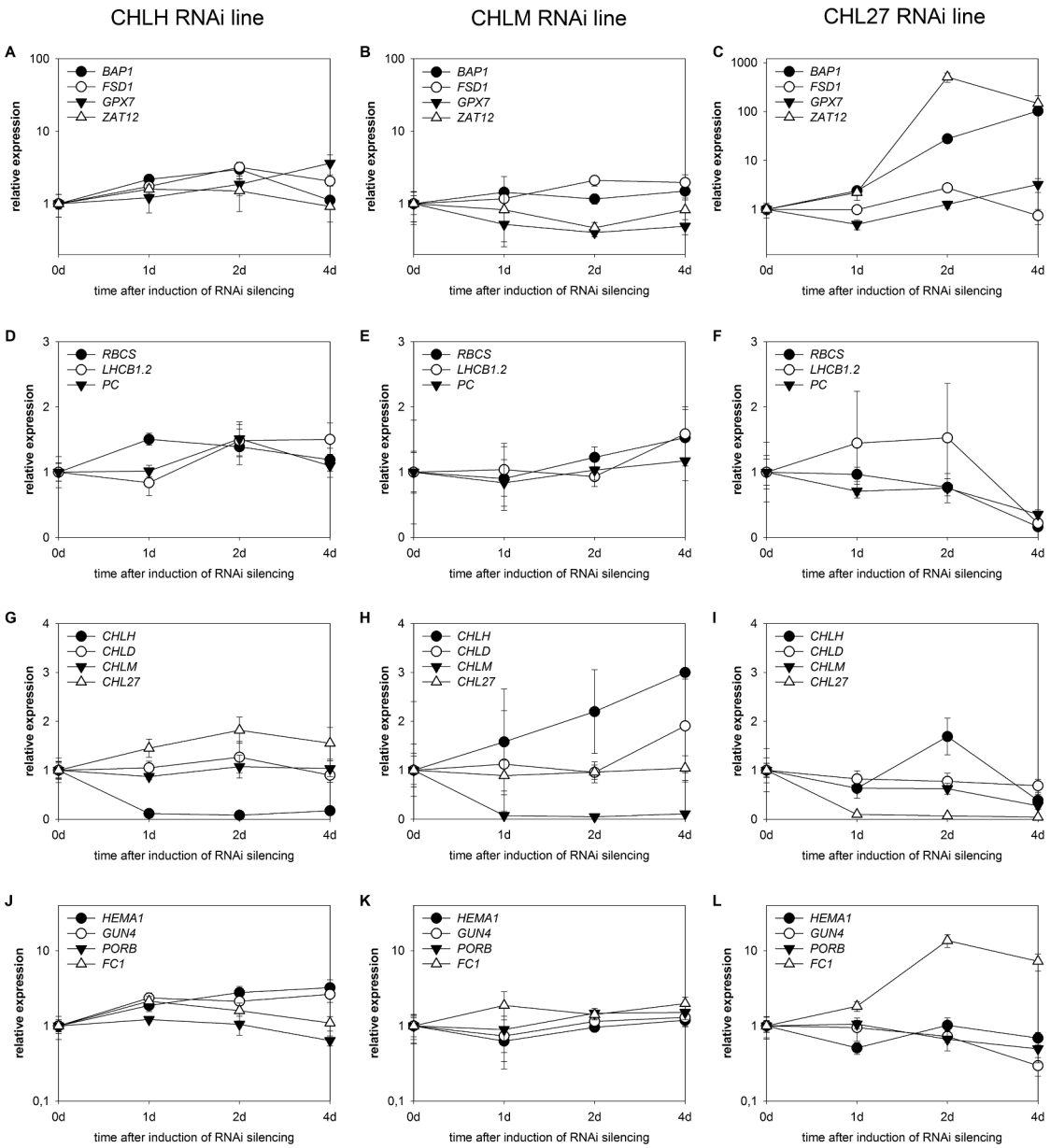

Figure 4 Analysis of the Transcript Levels of Nuclear Genes in the CHLH, CHLM, and CHL27 RNAi Lines during a Time Course of 4-d Induction of RNAi.

(A–C) Transcript analysis of ROS marker genes. *BAP1* a $^1O_2$-responsive gene and *ZAT12* a H_2O_2-responsive gene encoding bonzai1-associated protein 1 and zinc finger protein, respectively. *GPX7* and *FSD1* encode the plastid-localized glutathione peroxidase 7 and Fe-superoxide dismutase, respectively.

(D–F) Transcript analysis of the representatives of PhANGs, *RBCS*, *LHCB1.2*, and *PC* encoding ribulose 1,5-bisphosphate carboxylase small subunit, LHCB of photosystem II, and plastocyanin, respectively.

(G–I) Analysis of mRNA amounts of genes encoding enzymes of the Mg branch of tetrapyrrole biosynthesis. *CHLH* and *CHLD* encode the CHLH and CHLD subunit of Mg chelatase. *CHLM* and *CHL27* encode MgP methyltransferase and the CHL27 subunit of MgPME cyclase, respectively.

(J–L) Analysis of mRNA amounts of genes encoding target proteins of tetrapyrrole biosynthesis. *HEMA1*, *GUN4*, *PORB*, and *FC1* encode the glutamyl-tRNA reductase 1, GUN4, a positive regulator of the Mg chelatase reaction, protochlorophyllide oxidoreductase B, and ferrochelatase 1, respectively. Transcript levels were calculated as relative expression ($2^{-\Delta\Delta CT}$) according to Livak and Schmittgen (2001) in comparison to t_0 and *Actin2* as a reference gene. Data are given as means and SD of three biological replicates summarized in Supplemental Table 8. Plants were grown on MS for 14 d under continuous light (100 μmol photon m^{-2} s^{-1}).

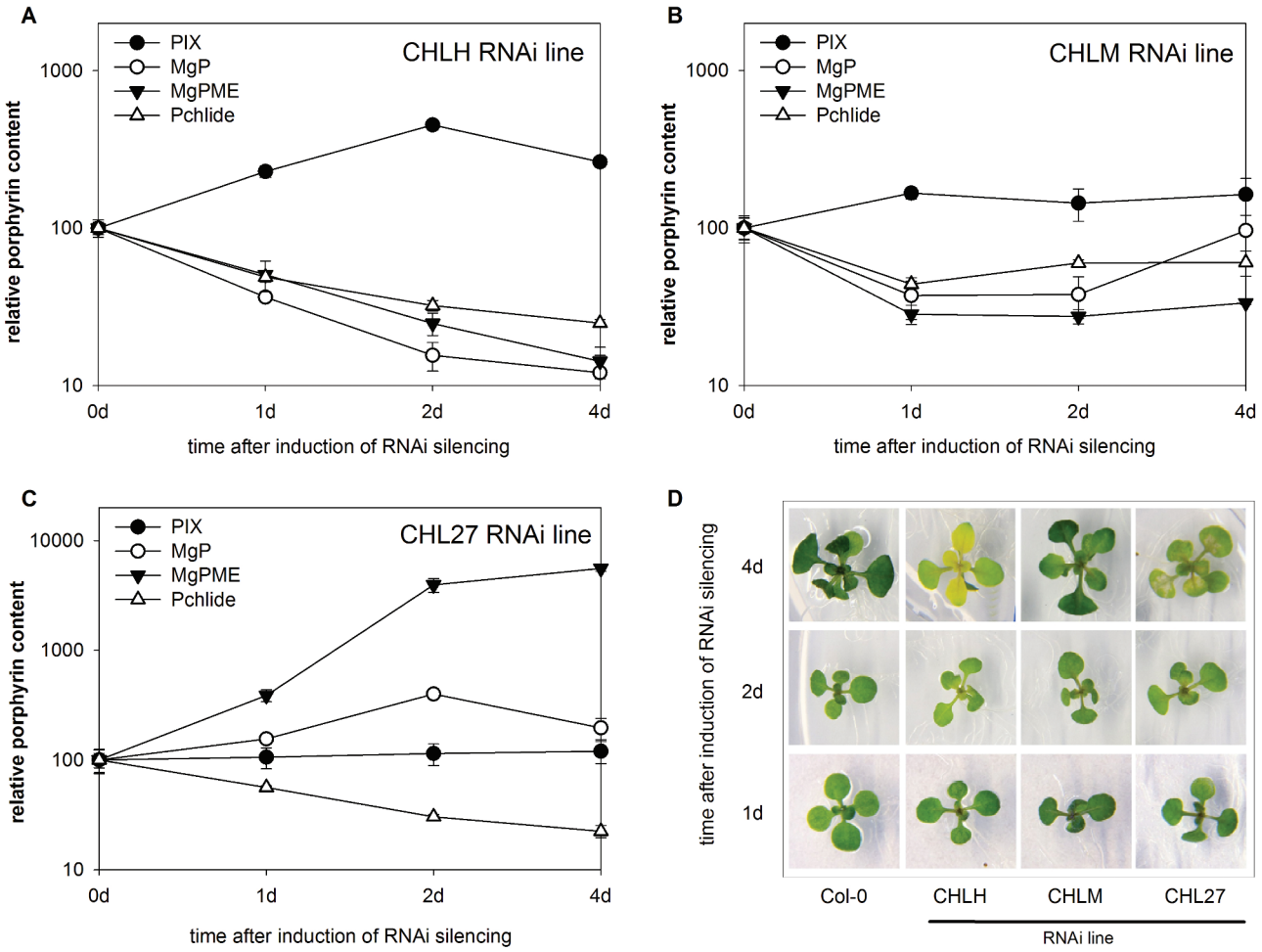

Figure 5 Kinetics on Steady-State Levels of PIX and Mg Porphyrins within a 4-d Silencing of Genes Encoding Proteins of Chlorophyll Biosynthesis.

(A–C) Time course of porphyrin steady-state levels 1, 2, and 4 d after induced RNAi gene silencing of *CHLH*, *CHLM*, and *CHL27* compared to the time point t_0. PIX, protoporphyrin, MgP, magnesium protoporphyrin, MgPME, MgP monomethylester, and Pchlide, protochlorophyllide were analyzed.

(D) Phenotypes of *Arabidopsis* wild-type and RNAi lines seedlings growing in continuous light of 100 µmol photon m^{-2} s^{-1} after a long-term dexamethasone-induced *CHLH*, *CHLM*, or *CHL27* gene silencing.

4-d period (Figure 4D and 4E), compared to the corresponding transcript levels in wild-type, while the transcript pattern of these three genes differed in the CHL27 RNAi line (Figure 4F). After 4 d of *CHL27* silencing, the mRNA levels of PhANGs were drastically decreased and correlated with the formation of necrotic leaf tissue triggered most likely by photooxidative damage of accumulating Mg porphyrins (Figure 6C).

Within 4 d of gene deactivation, the transcript accumulation of genes involved in the tetrapyrrole biosynthesis varied among the three RNAi lines (Figure 4G–4L). *FERROCHELATASE 1* (*FC1*) was the strongest up-regulated gene after 2 d of *CHL27* deactivation and indicates oxidative stress (Figure 4L), as it was previously reported (Nagai et al., 2007). The CHLH RNAi line showed slightly elevated transcript levels of *HEMA1* and *GUN4* (3.5- and 3.0-fold, respectively) after 4 d of *CHLH* deactivation (Figure 4J) and the CHLM RNAi line a 4.8-fold increase of *CHLH* mRNA (Figure 4H). In agreement with our findings, the *CHLH* mRNA was accumulating in a *chlm* knockout mutant (Pontier et al., 2007). But, in general, the regulation of the tetrapyrrole biosynthesis genes in the CHLH RNAi and CHLM RNAi line were barely altered more than two-fold in comparison to wild-type. In conclusion, the transcript levels of genes encoding enzymes of ALA synthesis and the Mg branch tend to elevate during *CHLH* and *CHLM* silencing, while they were down-regulated within 4 d of *CHL27* deactivation.

To determine the role of ROS in response to impaired chlorophyll biosynthesis, we analyzed transcripts of ROS marker genes, such as *BONZAI1-ASSOCIATED PROTEIN*

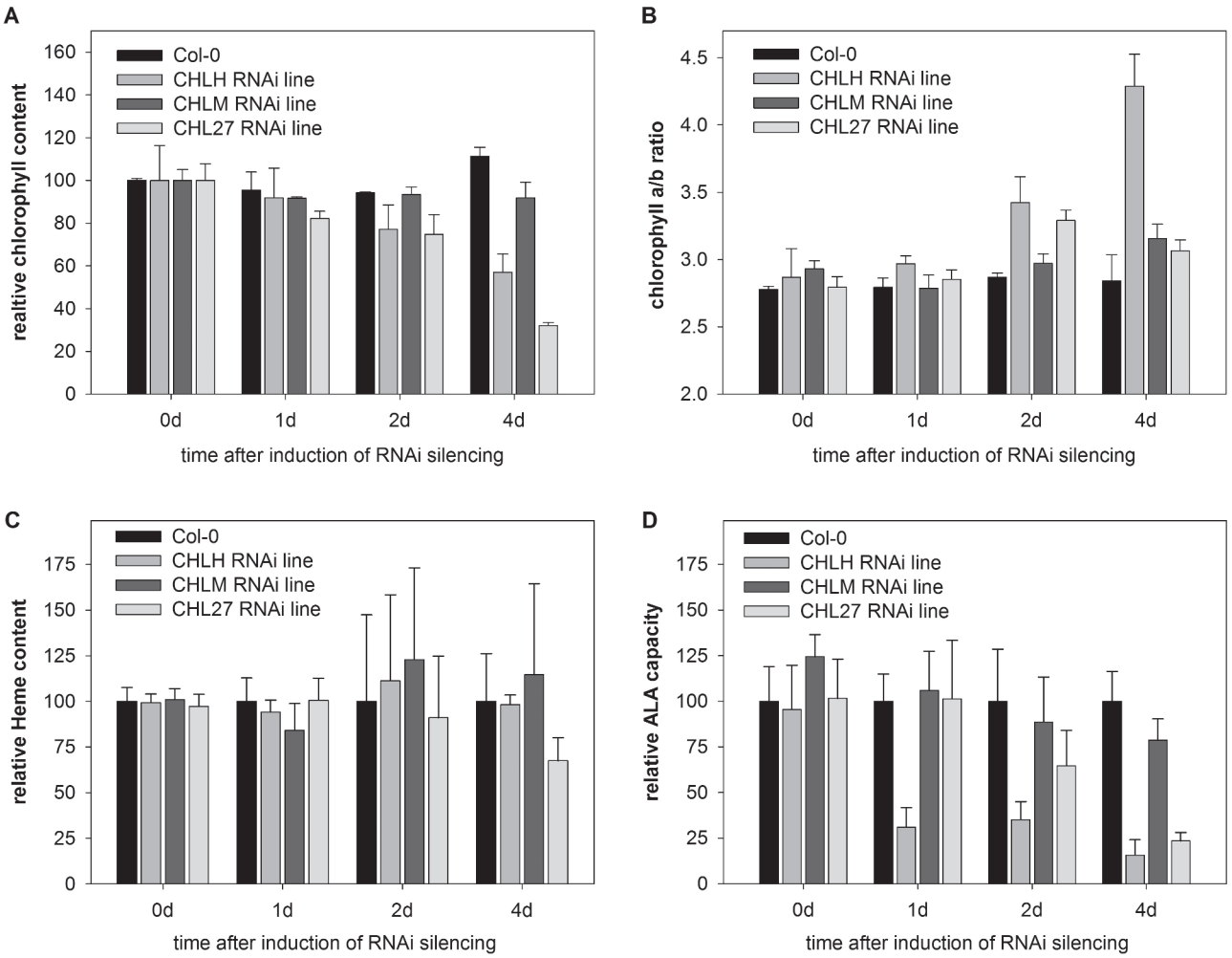

Figure 6 Analysis of Chlorophyll and Heme Content as well as ALA Capacity in Wild-Type and Transgenic RNAi Lines in the Course of 4-d Deactivation of Early Enzymatic Steps in the Mg Branch of Tetrapyrrole Biosynthesis.

(A) Relative chlorophyll content compared to time point t_0 for each line. The wild-type chlorophyll content at time point t_0 is 12.2 nmol mg^{-1} dw.

(B) The chlorophyll *a*/chlorophyll *b* ratio in wild-type and the three RNAi lines.

(C) Relative heme content in of transgenic lines compared to wild-type for each time point. The wild-type has a heme content of 1.2 pmol mg^{-1} dw at t_0. The heme content is not significantly altered in the RNAi lines within the 4 d of gene inactivation.

(D) ALA synthesizing capacity of the three RNAi lines compared to wild-type for each time point. The t_0 value of wild-type corresponds to 0.36 nmol ALA mg^{-1} fw h^{-1}.

(*BAP1*), a $^1O_2$-responsive gene (op den Camp et al., 2003), *ZAT12*, a H_2O_2-responsive gene (Rizhsky et al., 2004), *FSD1* encoding plastid-localized Fe-superoxide dismutase 1 (Pulido et al., 2010), and *GPX7* encoding the plastid-localized glutathione peroxidase 7 (Mullineaux et al., 2000). The transcript levels of *GPX7* and *BAP1* increased more than two-fold in the CHLH RNAi line after 2 and 4 d of *CHLH* silencing (Figure 4A). While the expression of the ROS marker genes remained stable in the CHLM RNA line, in the CHL27 RNAi line, the transcripts of *BAP1* and *ZAT12* accumulated substantially to more than 10-fold and 100-fold, respectively, and also *GPX7* mRNA content, although to a lesser extent, was also elevated (Figure 4C).

DISCUSSION

The synthesis of tetrapyrroles in plants depends on a tight control that follows the developmental program and demands of various environmental conditions, and is coordinated with production of apoproteins as well as the subsequent assembly of tetrapyrroles and proteins. Coordination of these processes is also ensured by a

constant plastid-derived operational control (Pogson et al., 2008). Among multiple plastid-localized metabolites and regulatory mechanisms, which have been reported to emit retrograde signals, Mg porphyrins were suggested to act as retrograde signals to thereby control NGE (Strand et al., 2003). However, despite the broad range of proposed retrograde signaling components, very little is known about the significance of each molecule operating as a signal in the proposed signaling pathways.

In an effort to expand our understanding of tetrapyrrole-mediated signaling, we have studied the immediate (short-term) impact of modified tetrapyrrole biosynthesis on NGE, while interference of other signals, such as ROS, photosynthetic redox control, and altered chlorophyll content, can be neglected. In compliance with the concept of permanent operational control by retrograde signals (Pogson et al., 2008; Estavillo et al., 2012), impaired plastid functions are expected to specifically emit and modulate retrograde signals exerting changes in NGE. Thus, with respect to tetrapyrrole biosynthesis, a specific inactivation of single metabolic steps in the pathway should instantaneously release retrograde signal(s).

To eliminate pleiotropic side effects from other signaling pathways, the dexamethasone-inducible pOpOff2 vector system (Wielopolska et al., 2005; Moore et al., 2006) was used to enable a short-term deactivation of the *CHLH*, *CHLM*, and *CHL27* expression. We showed that a 24-h-induced gene silencing evidently promoted a substantial reduction of activities of Mg chelatase, MgP methyltransferase, and MgPME cyclase, respectively (Figure 1C–1E). Misbalanced steady-state levels of Mg porphyrins were observed (Figure 2B and 2C), but no detectable effects on chlorophyll content were determined (Figure 2D). Deduced from seedling phenotype and chlorophyll content, it is likely that, during the early phase of RNAi gene silencing, photosynthesis and other physiological processes in the plastids were fully functional in the developed leaf cells.

Using a comparative microarray approach, we showed that the short-term gene silencing of *CHLH*, *CHLM*, and *CHL27* leads to an up- or down-regulation of 206, 188, and 206 genes, respectively. In this context, it is important to note that most of these transcripts are solely regulated in response to the inducible RNAi vector system as it was shown by using the LUC RNAi control line (Figure 3). It is known that the used RNAi system did not affect a broad range of physiological and morphological parameters (Huang et al., 2011). Nevertheless, further investigations could find out whether either the overexpression of siRNA due to the induction of the inducible RNAi vector system or a direct modification of *Arabidopsis* gene expression caused by the dexamethasone-activated transcription factor itself are responsible for the observed changes of NGE.

The results of the transcriptome analysis obtained after short-term modified metabolic activity of the early steps in the Mg branch of tetrapyrrole biosynthesis contradict an instantaneous modulation of NGE. Among the few genes which are deregulated either commonly among the induced RNAi lines or exclusively in one of the transgenic lines, no gene was found which encodes a protein with a putative or established function in chloroplast or intracellular communication in response to plastid damages in wild-type or in mutants of plastid retrograde signaling (Supplemental Tables 1 and 4). The potential functions of these conspicuous genes of our transcriptome analysis could not be correlated with classes of genes required for responses to plastid damage, or modified metabolic activities in plastids. No PhANGs or genes encoding tetrapyrrole biosynthesis-associated proteins were identified among the deregulated genes after 24 h of induced RNAi inactivation (Supplemental Table 1).

Although changes of steady-state levels of PIX and Mg porphyrins were observed within 24 h of gene silencing for enzymes of the Mg branch, changes of NGE in an immediate response of the accumulation of tetrapyrrole intermediates and their modified steady-state levels could not be observed. These results are consistent with previous analyses, when no specific and unidirectional correlation between MgP accumulation and *LHCB1.2* expression was determined (Mochizuki et al., 2008; Moulin et al., 2008). Thus, independent short-term deactivation of the first three enzymes of the Mg branch seems not to be directly involved in retrograde signaling. Importantly, when metabolic changes in the tetrapyrrole biosynthesis pathway were observed (Figure 2B and 2C), then regulatory consequences, such as reduced ALA synthesis (Figure 2E), can already be measured. Due to high plasticity of chloroplasts, the short-term reduction of enzyme activities of the three first enzymatic steps of the Mg branch is apparently balanced in the entire pathway by posttranslational mechanisms. As long as deactivation of enzyme activities does not affect chlorophyll content or activate ROS signaling pathways caused by porphyrin accumulation, retrograde signaling in response to Mg porphyrin biosynthesis is not specifically modulated and, in consequence, distinct changes of transcript levels of nuclear genes are not induced.

These observations challenge the prevailing view that PIX and, in particular, Mg porphyrins are retrograde signals and tetrapyrrole metabolism at the stages of Mg porphyrin synthesis contributes to the plastid-derived signaling (Strand et al., 2003; McCormac and Terry, 2004; Kindgren et al., 2012). Many reports on plant tetrapyrrole-derived signaling are based on analysis of either constitutive mutants impaired in tetrapyrrole biosynthesis, which are or are not additionally treated with exogenous inhibitors, such as norflurazon. These studies were performed at early stages of seedling development and exemplified as

biogenic control (Pogson et al., 2008), but it was not possible to differentiate between induced tetrapyrrole- and ROS-dependent retrograde signaling. On the contrary, the inducible gene deactivation system expressed in green seedlings enabled us not only to explore the effects of potential emitters of retrograde signals exerting changes in NGE over the first hours and days following specific modulations of tetrapyrrole metabolism, but also provided sufficient amounts of plant tissue for genetic and biochemical analyses.

Long-Term Response to Induced Deactivation of Enzymatic Steps in Chlorophyll Biosynthesis

As significant transcriptional changes of nuclear genes for tetrapyrrole biosynthesis-related proteins were not determined within the first 24 h of induced *CHLH*, *CHLM*, and *CHL27* silencing, we aimed to examine time-resolved changes in NGE in response to a deactivated Mg branch. After long-term RNAi-mediated gene silencing, two different phenotypes could be differentiated among the transgenic lines in response to perturbed tetrapyrrole biosynthesis. In response to deactivated gene expression and reduced enzyme activity (Figure 1A, 1C, and 1D), the CHLH RNAi line and, to a lesser extent, the CHLM RNAi line represented pale-green mutants (Figure 5D) with reduced levels of metabolic products of the Mg branch (Figure 5A and 5B). These lines are characterized by an attenuated metabolic flow of the pathway into the Mg branch. In contrast, the CHL27 RNAi line accumulated phototoxic MgPME levels, which ultimately caused leaf necroses (Figure 5C and 5D).

The steady-state levels of PIX and Mg porphyrins in response to inactivated *CHLH*, *CHLM*, and *CHL27* expression reflect the modified control of the metabolic flow in the tetrapyrrole biosynthesis pathway, but do not necessarily correlate with potential retrograde signaling. A decelerated metabolic flow in response to *CHLH* and *CHLM* inactivation minimized the content of the products of these two enzymatic steps, while *CHL27* deactivation correlated instantaneously with the increasing contents of MgPME.

To date, retrograde signaling studies with mutant seedlings are aimed to elucidate potential roles and action mechanisms of the components of plastid-derived signaling, mainly during the acclimation to stress. The experimental strategy for the exploration of the mutants with defective genes encoding proteins of tetrapyrrole biosynthesis hampered the distinction between tetrapyrrole-mediated and other retrograde signaling pathways, including ROS- and redox-induced signaling, and led to pleiotropic phenotypes of bleaching or necroses of leaves and growth inhibition (Meskauskiene et al., 2001; Mochizuki et al., 2001; Larkin et al., 2003; Strand et al., 2003). We are aware that the effects of accumulating Mg porphyrins cannot ultimately be discussed without considering their photoreactive properties and, in consequence, their crosstalk with other retrograde signaling pathways during light exposure (Nott et al., 2006; Pogson et al., 2008). Using the inducible RNAi system for three different enzymatic steps of the tetrapyrrole pathway, primary effects can be separated from secondary effects using time-resolved analyses as demonstrated here.

Considering the diverse phenotypes of the pale-green CHLH RNAi and CHLM RNAi lines versus the necrotic CHL27 RNAi line, the pattern of induced changes in NGE in each transgenic line correlated with either the distinct phenotype of reduced leaf pigmentation or necrotic leaf lesions. Each representative of the PhANGs as well as tetrapyrrole biosynthesis and ROS marker genes did not reveal similar kinetics during the 4-d deactivation of either *CHLH*, *CHLM*, or *CHL27*; instead, each analyzed gene indicated individual regulation of transcript accumulation (Figure 4). Four-day deactivation of *CHLH* and *CHLM* caused a slight accumulation of the *LHCB1.2*, *RBSC*, and *PC* mRNA levels (Figure 4D and 4E), while their transcript contents drastically decreased in the CHL27 RNAi line after 2 d of gene silencing compared to t_0 (Figure 4F).

An induction of typical ROS marker genes was determined after 2 and 4 d following *CHL27* silencing (Figure 4C) indicating an increasing oxidative stress rather than a tetrapyrrole biosynthesis-specific control. However, *GPX7* and *FSD1* normally responded to production of hydrogen peroxide (Mullineaux et al., 2000) and superoxide (Pulido et al., 2010) and were less induced than *ZAT12* and *BAP1* in the CHL27 RNAi line. *BAP1* is known as singlet oxygen ($^1O_2$)-responsive gene (op den Camp et al., 2003). We suggest that the excessive MgPME accumulation in light-exposed seedlings (after 1 d; Figure 2C) generates $^1O_2$, which induces ROS-mediated retrograde signaling leading to induction of ROS marker genes (2 d; Figure 4C) and suppression of PhANGs and tetrapyrrole biosynthesis genes (Figure 4F, 4I, and 4L). These processes presumably resemble consequences of Pchlide accumulation in light-dark grown *flu* mutants (Meskauskiene et al., 2001) and it is hypothesized that the pattern of modified NGE of the long-term inactivated CHL27 RNA line is similar to $^1O_2$-induced *flu* transcriptome (op den Camp et al., 2003). In contrast to RNAi-mediated *CHL27* inactivation, none of the investigated ROS-responsive transcripts accumulated after *CHLH* and *CHLM* deactivation (Figure 4A and 4B).

The *Arabidopsis* CHLH RNAi and CHLM RNAi lines resemble transgenic tobacco plants expressing either *CHLH* or *CHLM* antisense RNA (Papenbrock et al., 2000; Alawady and Grimm, 2005). In agreement with these reports, inactivation of the first two enzymes of the Mg branch results in suppression of ALA synthesis (Figure 6D) and, consequently, lower PIX and Mg porphyrin contents. The altered transcript levels of PhANGs and genes of tetrapyrrole

biosynthesis upon the long-term *CHLH* and *CHLM* deactivation is associated with reduced chlorophyll content, impaired photosynthesis, and/or reduced feed-controlled ALA biosynthesis. Future studies are necessary to verify the multiple retrograde signals which are derived from ALA synthesis, chlorophyll deficiency, and diminished photosynthesis capacity and contribute to the control of NGE. In this context, two independent sets of *Arabidopsis* seedlings with reduced ALA synthesis contain an overlapping class of deregulated genes: the *gun4-1* knockdown mutant and seedlings upon inhibition of gabaculine (inhibitor of glutamate 1-semialdehyde aminotransferase, the second enzyme of ALA biosynthesis) (Czarnecki et al., 2012). It can be hypothesized that long-term inactivation of Mg chelatase and MgProto methyltransferase deregulates an overlapping set of genes similarly to direct reduction of ALA synthesis.

In contrast, short-term inactivated *CHL27* expression tends to stimulate ALA biosynthesis, as previously reported in response to reduced expression of the cyclase subunit LCAA/YCF54 (Albus et al., 2012). But, after 2 d of induced gene deactivation, ALA biosynthesis is down-regulated. The induced ROS marker genes and the necrotic leaf spots are indicative for photooxidative stress after 2 d of *CHL27* deactivation (Figure 4C). Experimental evidence for oxidative stress-inactivated ALA biosynthesis has been previously presented (Aarti et al., 2007).

The heme content in all three transgenic lines was not altered during the investigation period in comparison to wild-type, although the metabolic flow in tetrapyrrole biosynthesis was substantially affected by deactivation of the enzymatic steps in chlorophyll biosynthesis. An inhibitory effect of heme on the ALA synthesis rate at the post-translational level was proposed previously (Pontoppidan and Kannangara, 1994; Srivastava et al., 2005). Moreover, *Arabidopsis* ferrochelatase 1 overexpressor lines accumulate more PhANGs upon norflurazon inhibition than wild-type and heme synthesis is proposed to be associated with up-regulation of PhANGs (Woodson et al., 2011). Therefore, the existence of further regulatory mechanisms affecting the rate-limiting steps of ALA formation by the transcriptional and posttranslational control is likely and these can be mediated by regulatory heme pools and chlorophyll availability.

In conclusion, NGE deregulation in response to deactivation of enzymatic steps of chlorophyll biosynthesis and changes in Mg porphyrin levels is only observed after more than 1 d of gene deactivation and follows different regulatory mechanisms, which are specific for the inactivated step. Changes in NGE by *CHLH* and *CHLM* deactivation correlate with reduced chlorophyll content and attenuated metabolic flow in the tetrapyrrole biosynthetic pathway. Long-term *CHL27* deactivation induces the expression of genes by a ROS-dependent signaling pathway, while PhANGs and genes of tetrapyrrole biosynthesis tend to be down-regulated. These changes correlate with transcriptional control of NGE in response to MgPME-induced $^1O_2$ formation (Laloi et al., 2007). It will be important in future to pay attention to the integration of different retrograde signaling pathways, which are triggered by metabolites and environmental signals in chloroplast and induce collectively NGE.

METHODS

Biological Material, Growth Conditions, and Treatment

To generate dexamethasone-inducible RNAi pOpOff2 lines, specific sequences of the corresponding coding regions (Supplemental Table 6) were cloned into pDONR221 (Invitrogen). The target fragments were subsequently recombined into the destination vector pOpOff2(hyg) (Wielopolska et al., 2005) using the GATEWAY™ system (Invitrogen). After *Agrobacterium*-mediated transformation, seeds of the F1 generation of CHLH RNAi, CHLM RNAi, and CHL27 RNAi lines were selected on MS plates containing hygromycin (35 μg ml^{-1}). The LUC RNAi line targets the firefly luciferase and was previously introduced including the description of potential secondary effects of the RNAi system used (Huang et al., 2011). The RNAi system includes inter alia, a gene encoding a constitutively expressed chimeric transcription factor, which binds with dexamethasone to the pOp6 promoter for expression of RNAi cassette.

The *Arabidopsis* wild-type (Col-0) and transgenic RNAi lines were grown on soil at 110 μmol photons m^{-2} s^{-1} under short-day (10-h light) conditions, acclimated for at least 3 d in continuous light and sprayed with dexamethasone (20 μg ml^{-1}). The kinetic data are generated from 14-day-old seedlings grown on MS medium at 100 μmol photons m^{-2} s^{-1} continuous light, and subsequently transferred to dexamethasone (20 μg ml^{-1}) containing MS plates.

Extraction and HPLC Analysis of Porphyrins and Pigments

Samples from wild-type and transgenic seedlings were frozen, homogenized with a ball mill, and freeze-dried. Powdered samples were suspended in ice-cold acetone/0.1 M NH_4OH (9/1, v/v), centrifuged, and analyzed. Chlorophyll, heme, and tetrapyrrole metabolites were analyzed according to Kim et al. (2013) and PIX according to Scharfenberg et al. (2013). MgP and MgPME were separated on a Poroshell 120 EC-C18 (Agilent) column (2.7 μm; 150 × 3.0 mm; 21°C) at a flow rate of 0.55 ml min^{-1} and isocratic eluted with 90% of solvent A (90% methanol; 10% 1 M ammonium acetate pH 7.0) and 10% of solvent B (100% ethyl acetate). Porphyrins were quantified at

λ_{Ex} 420 nm and λ_{Em} 600 nm (peak width 2.31 Hz; PMT gain 17) using authentic standards.

ALA Synthesis Capacity

Arabidopsis seedlings were harvested after treatment with dexamethasone, incubated for 4 h in 40 mM levulinic acid and TRIS/HCL buffer (pH 7.2) and analyzed according to Mauzerall and Granick (1956) with modifications (Richter et al., 2013). Frozen samples were ground in a ball mill, re-suspended in 20 mM potassium phosphate buffer (pH 6.8), and centrifuged. Four hundred µl of the supernatant was mixed with 100 µl ethyl acetoacetate, boiled for 10 min, and chilled to room temperature. After adding modified Ehrlich's reagent, the absorption of the ALA pyrrole was measured at 553 nm. ALA quantification based on at least three biological replicates using a standard curve of ALA.

Transcript Analysis

Total RNA was extracted from *Arabidopsis* seedlings using TRIsure reagent (Bioline) and 2 µg RNA was used for DNase treatment and reverse transcription (Thermo Fisher Scientific) using oligo-dT_{18} following the manufacturer's protocol. The qRT–PCR was performed using SensiMix (Bioline) and a BFX96 thermo cycler (Biorad) with the following program: 10 min at 95°C, 45 cycles of 15 s at 95°C, 15 s at 60°C, and 15 s at 72°C. Calculation of relative expression levels was performed according to Livak and Schmittgen (2001) using *AtACT2* (At3g18780) as reference genes. Supplemental Table 7 shows the primer pairs used for transcript analysis.

Microarray Analysis, Data Normalization, Differential Expression, and Heat Map

Microarray analysis was performed using the ATH1 Arabidopsis Gene Chip. The quality control of RNA and hybridization was performed at Nottingham Arabidopsis Stock Centre (UK). Analysis of differential expression was conducted using the LIMMA package (Smyth, 2004) and Bioconductor (Gentleman et al., 2004) in R. Affymetrix spots were translated to TAIR10 annotation using the cdf file provided by http://nmg-r.bioinformatics.nl/NuGO_R.html. Expression was calculated by applying the function just.rma with standard settings (robust multi-array average expression measure, RMA) (Irizarry et al., 2003) as background correction, quantile normalization, and differential expression calculation was subsequently carried out using an empirical Bayes linear modeling approach. The resulting *p*-values were corrected according to Benjamini and Hochberg (1995). Genes were considered to be significantly deregulated when their respective *p*-value was ≤0.05 and the fold change was two-fold. All genes being differentially expressed were depicted in a heat map using function heatmap.2 implemented in the R stats package. The scaling was based on rows, thus left at default, while the colors were set to an interpolation of blue and yellow.

Chloroplast Isolation and Enzyme Activity Assays

Chloroplasts were extracted from 3–4-week-old seedlings grown on soil and treated with dexamethasone for 24 h. The plant material was homogenized in pre-cooled extraction buffer (0.8 M sorbitol, 40 mM Tricine-KOH; pH 8.0; 20 mM $NaHCO_3$, and 0.2% bovine serum albumin (BSA), filtered through Miracloth (Merck Millipore), centrifuged at 500 *g* for 8 min, and the pellet was re-suspended in extraction buffer without (BSA). The crude chloroplast extracts were used for enzyme activity measurements using the assay buffer (0.8 M sorbitol, 40 mM Tricine-KOH; pH 8.0; 20 mM $NaHCO_3$, 25 mM $MgCl_2$, 1 mM DTT, and 0.2% BSA). The Mg chelatase activity was assayed with modifications as previously described (Peter and Grimm, 2009). The chloroplast extract was mixed with an equal volume of assay buffer and 16 mM ATP and 20 µM PIX, 800 r.p.m., 30°C, in darkness. After centrifugation, the MgP content was measured via HPLC analysis as described above. The protocol of the methyltransferase assay was adapted from Richter et al. (2013), whereas the assay buffer is supplemented with 1 mM S-adenosyl-methionine and 40 µM MgP. For the cyclase assay, 10 mM NADPH and 12 µM MgPME were added. For enzyme assays, the catalytic product was quantified using tetrapyrrole standards (see above), except for the cyclase assay, when the rate of metabolized substrate was measured.

SUPPLEMENTARY DATA

Supplementary Data are available at *Molecular Plant Online.*

FUNDING

This work was supported by grants of the Deutsche Forschungsgemeinschaft (FOR 804).

ACKNOWLEDGMENTS

We would like to thank Ian Moore (Oxford University, UK) for providing the pOpOff2(kan)::LUC control transgenic line. We thank Pawel Brzezowski and Boris Hedtke for critically reading the manuscript. No conflict of interest declared.

REFERENCES

Aarti, D., Tanaka, R., Ito, H., and Tanaka, A. (2007). High light inhibits chlorophyll biosynthesis at the level of 5-aminolevulinate synthesis during de-etiolation in cucumber (*Cucumis sativus*) cotyledons. Photochem. Photobiol. **83**, 171–176.

Abdallah, F., Salamini, F., and Leister, D. (2000). A prediction of the size and evolutionary origin of the proteome of chloroplasts of *Arabidopsis*. Trends Plant Sci. **5**, 141–142.

Alawady, A.E., and Grimm, B. (2005). Tobacco Mg protoporphyrin IX methyltransferase is involved in inverse activation of Mg porphyrin and protoheme synthesis. Plant J. **41**, 282–290.

Albus, C.A., Salinas, A., Czarnecki, O., Kahlau, S., Rothbart, M., Thiele, W., Lein, W., Bock, R., Grimm, B., and Schottler, M.A. (2012). LCAA, a novel factor required for magnesium protoporphyrin monomethylester cyclase accumulation and feedback control of aminolevulinic acid biosynthesis in tobacco. Plant Physiol. **160**, 1923–1939.

Apel, K., and Hirt, H. (2004). Reactive oxygen species: metabolism, oxidative stress, and signal transduction. Annu. Rev. Plant Biol. **55**, 373–399.

Baier, M., and Dietz, K.J. (2005). Chloroplasts as source and target of cellular redox regulation: a discussion on chloroplast redox signals in the context of plant physiology. J. Exp. Bot. **56**, 1449–1462.

Benjamini, Y., and Hochberg, Y. (1995). Controlling the false discovery rate: a practical and powerful approach to multiple testing. J. Roy. Stat. Soc. Ser. B. **6**, 1580–1591.

Brautigam, K., Dietzel, L., Kleine, T., Stroher, E., Wormuth, D., Dietz, K.J., Radke, D., Wirtz, M., Hell, R., Dormann, P., et al. (2009). Dynamic plastid redox signals integrate gene expression and metabolism to induce distinct metabolic states in photosynthetic acclimation in *Arabidopsis*. Plant Cell. **21**, 2715–2732.

Chi, W., Sun, X., and Zhang, L. (2013). Intracellular signaling from plastid to nucleus. Annu. Rev. Plant Biol. **64**, 559–582.

Cornah, J.E., Terry, M.J., and Smith, A.G. (2003). Green or red: what stops the traffic in the tetrapyrrole pathway? Trends Plant Sci. **8**, 224–230.

Czarnecki, O., and Grimm, B. (2012). Post-translational control of tetrapyrrole biosynthesis in plants, algae, and cyanobacteria. J. Exp. Bot. **63**, 1675–1687.

Czarnecki, O., Glasser, C., Chen, J.G., Mayer, K.F., and Grimm, B. (2012). Evidence for a contribution of ALA synthesis to plastid-to-nucleus signaling. Frontiers in Plant Science. **3**, 236.

Eden, E., Navon, R., Steinfeld, I., Lipson, D., and Yakhini, Z. (2009). GOrilla: a tool for discovery and visualization of enriched GO terms in ranked gene lists. BMC Bioinformatics. **10**, 48.

Estavillo, G.M., Chan, K.X., Phua, S.Y., and Pogson, B.J. (2012). Reconsidering the nature and mode of action of metabolite retrograde signals from the chloroplast. Frontiers in Plant Science. **3**, 300.

Estavillo, G.M., Crisp, P.A., Pornsiriwong, W., Wirtz, M., Collinge, D., Carrie, C., Giraud, E., Whelan, J., David, P., Javot, H., et al. (2011). Evidence for a SAL1–PAP chloroplast retrograde pathway that functions in drought and high light signaling in *Arabidopsis*. Plant Cell. **23**, 3992–4012.

Galvez-Valdivieso, G., and Mullineaux, P.M. (2010). The role of reactive oxygen species in signalling from chloroplasts to the nucleus. Physiol Plant. **138**, 430–439.

Gentleman, R.C., Carey, V.J., Bates, D.M., Bolstad, B., Dettling, M., Dudoit, S., Ellis, B., Gautier, L., Ge, Y., Gentry, J., et al. (2004). Bioconductor: open software development for computational biology and bioinformatics. Genome Biol. **5**, R80.

Gray, J.C., Sullivan, J.A., Wang, J.H., Jerome, C.A., and MacLean, D. (2003). Coordination of plastid and nuclear gene expression. Philos. Trans. R Soc. Lond. B Biol. Sci. **358**, 135–144; discussion 144–135.

Hruz, T., Laule, O., Szabo, G., Wessendorp, F., Bleuler, S., Oertle, L., Widmayer, P., Gruissem, W., and Zimmermann, P. (2008). Genevestigator v3: a reference expression database for the meta-analysis of transcriptomes. Advances in Bioinformatics. **2008**, 420747.

Huang, W., Ling, Q., Bedard, J., Lilley, K., and Jarvis, P. (2011). *In vivo* analyses of the roles of essential Omp85-related proteins in the chloroplast outer envelope membrane. Plant Physiol. **157**, 147–159.

Irizarry, R.A., Hobbs, B., Collin, F., Beazer-Barclay, Y.D., Antonellis, K.J., Scherf, U., and Speed, T.P. (2003). Exploration, normalization, and summaries of high density oligonucleotide array probe level data. Biostatistics. **4**, 249–264.

Joyard, J., Ferro, M., Masselon, C., Seigneurin-Berny, D., Salvi, D., Garin, J., and Rolland, N. (2009). Chloroplast proteomics and the compartmentation of plastidial isoprenoid biosynthetic pathways. Mol. Plant. **2**, 1154–1180.

Kim, C., and Apel, K. (2013). Singlet oxygen-mediated signaling in plants: moving from flu to wild type reveals an increasing complexity. Photosynth. Res. **116**, 455–464.

Kim, C., Meskauskiene, R., Apel, K., and Laloi, C. (2008). No single way to understand singlet oxygen signalling in plants. EMBO Rep. **9**, 435–439.

Kim, S., Schlicke, H., Van Ree, K., Karvonen, K., Subramaniam, A., Richter, A., Grimm, B., and Braam, J. (2013). *Arabidopsis* chlorophyll biosynthesis: an essential balance between the methylerythritol phosphate and tetrapyrrole pathways. Plant Cell. **25**, 4984–4993.

Kindgren, P., Noren, L., Lopez Jde, D., Shaikhali, J., and Strand, A. (2012). Interplay between Heat Shock Protein 90 and HY5 controls PhANG expression in response to the GUN5 plastid signal. Mol. Plant. **5**, 901–913.

Kropat, J., Oster, U., Rudiger, W., and Beck, C.F. (2000). Chloroplast signalling in the light induction of nuclear HSP70 genes requires

the accumulation of chlorophyll precursors and their accessibility to cytoplasm/nucleus. Plant J. **24**, 523–531.

Laloi, C., Stachowiak, M., Pers-Kamczyc, E., Warzych, E., Murgia, I., and Apel, K. (2007). Cross-talk between singlet oxygen- and hydrogen peroxide-dependent signaling of stress responses in *Arabidopsis thaliana*. Proc. Natl Acad. Sci. U S A. **104**, 672–677.

Larkin, R.M., Alonso, J.M., Ecker, J.R., and Chory, J. (2003). GUN4, a regulator of chlorophyll synthesis and intracellular signaling. Science. **299**, 902–906.

Leister, D. (2005). Origin, evolution and genetic effects of nuclear insertions of organelle DNA. Trends Genet. **21**, 655–663.

Lermontova, I., and Grimm, B. (2006). Reduced activity of plastid protoporphyrinogen oxidase causes attenuated photodynamic damage during high-light compared to low-light exposure. Plant J. **48**, 499–510.

Livak, K.J., and Schmittgen, T.D. (2001). Analysis of relative gene expression data using real-time quantitative PCR and the 2(-Delta Delta C(T)) Method. Methods. **25**, 402–408.

Martin, W., Rujan, T., Richly, E., Hansen, A., Cornelsen, S., Lins, T., Leister, D., Stoebe, B., Hasegawa, M., and Penny, D. (2002). Evolutionary analysis of *Arabidopsis*, cyanobacterial, and chloroplast genomes reveals plastid phylogeny and thousands of cyanobacterial genes in the nucleus. Proc. Natl Acad. Sci. U S A. **99**, 12246–12251.

Mauzerall, D., and Granick, S. (1956). The occurrence and determination of delta-amino-levulinic acid and porphobilinogen in urine. J. Biol. Chem. **219**, 435–446.

McCormac, A.C., and Terry, M.J. (2004). The nuclear genes Lhcb and HEMA1 are differentially sensitive to plastid signals and suggest distinct roles for the GUN1 and GUN5 plastid-signalling pathways during de-etiolation. Plant J. **40**, 672–685.

Meskauskiene, R., Nater, M., Goslings, D., Kessler, F., op den Camp, R., and Apel, K. (2001). FLU: a negative regulator of chlorophyll biosynthesis in *Arabidopsis thaliana*. Proc. Natl Acad. Sci. U S A. **98**, 12826–12831.

Mochizuki, N., Brusslan, J.A., Larkin, R., Nagatani, A., and Chory, J. (2001). *Arabidopsis* genomes uncoupled 5 (GUN5) mutant reveals the involvement of Mg-chelatase H subunit in plastid-to-nucleus signal transduction. Proc. Natl Acad. Sci. U S A. **98**, 2053–2058.

Mochizuki, N., Tanaka, R., Grimm, B., Masuda, T., Moulin, M., Smith, A.G., Tanaka, A., and Terry, M.J. (2010). The cell biology of tetrapyrroles: a life and death struggle. Trends Plant Sci. **15**, 488–498.

Mochizuki, N., Tanaka, R., Tanaka, A., Masuda, T., and Nagatani, A. (2008). The steady-state level of Mg-protoporphyrin IX is not a determinant of plastid-to-nucleus signaling in *Arabidopsis*. Proc. Natl Acad. Sci. U S A. **105**, 15184–15189.

Moore, I., Samalova, M., and Kurup, S. (2006). Transactivated and chemically inducible gene expression in plants. Plant J. **45**, 651–683.

Moulin, M., McCormac, A.C., Terry, M.J., and Smith, A.G. (2008). Tetrapyrrole profiling in *Arabidopsis* seedlings reveals that retrograde plastid nuclear signaling is not due to Mg-protoporphyrin IX accumulation. Proc. Natl Acad. Sci. U S A. **105**, 15178–15183.

Mullineaux, P., Ball, L., Escobar, C., Karpinska, B., Creissen, G., and Karpinski, S. (2000). Are diverse signalling pathways integrated in the regulation of *Arabidopsis* antioxidant defence gene expression in response to excess excitation energy? Philos. Trans. R Soc. Lond. B Biol. Sci. **355**, 1531–1540.

Nagai, S., Koide, M., Takahashi, S., Kikuta, A., Aono, M., Sasaki-Sekimoto, Y., Ohta, H., Takamiya, K., and Masuda, T. (2007). Induction of isoforms of tetrapyrrole biosynthetic enzymes, AtHEMA2 and AtFC1, under stress conditions and their physiological functions in *Arabidopsis*. Plant Physiol. **144**, 1039–1051.

Nott, A., Jung, H.S., Koussevitzky, S., and Chory, J. (2006). Plastid-to-nucleus retrograde signaling. Annu. Rev. Plant Biol. **57**, 739–759.

Oelmuller, R., and Mohr, H. (1986). Photooxidative destruction of chloroplasts and its consequences for expression of nuclear genes. Planta. **167**, 106–113.

op den Camp, R.G., Przybyla, D., Ochsenbein, C., Laloi, C., Kim, C., Danon, A., Wagner, D., Hideg, E., Gobel, C., Feussner, I., et al. (2003). Rapid induction of distinct stress responses after the release of singlet oxygen in *Arabidopsis*. Plant Cell. **15**, 2320–2332.

Papenbrock, J., and Grimm, B. (2001). Regulatory network of tetrapyrrole biosynthesis–studies of intracellular signalling involved in metabolic and developmental control of plastids. Planta. **213**, 667–681.

Papenbrock, J., Mock, H.P., Tanaka, R., Kruse, E., and Grimm, B. (2000). Role of magnesium chelatase activity in the early steps of the tetrapyrrole biosynthetic pathway. Plant Physiol. **122**, 1161–1169.

Pesaresi, P., Schneider, A., Kleine, T., and Leister, D. (2007). Interorganellar communication. Curr. Opin. Plant Biol. **10**, 600–606.

Peter, E., and Grimm, B. (2009). GUN4 is required for posttranslational control of plant tetrapyrrole biosynthesis. Mol. Plant. **2**, 1198–1210.

Pfannschmidt, T., Brautigam, K., Wagner, R., Dietzel, L., Schroter, Y., Steiner, S., and Nykytenko, A. (2009). Potential regulation of gene expression in photosynthetic cells by redox and energy state: approaches towards better understanding. Ann. Bot. **103**, 599–607.

Pogson, B.J., Woo, N.S., Forster, B., and Small, I.D. (2008). Plastid signalling to the nucleus and beyond. Trends Plant Sci. **13**, 602–609.

Pontier, D., Albrieux, C., Joyard, J., Lagrange, T., and Block, M.A. (2007). Knock-out of the magnesium protoporphyrin IX methyltransferase gene in *Arabidopsis*: effects on chloroplast

development and on chloroplast-to-nucleus signaling. J. Biol. Chem. **282**, 2297–2304.

Pontoppidan, B., and Kannangara, C.G. (1994). Purification and partial characterisation of barley glutamyl-tRNA(Glu) reductase, the enzyme that directs glutamate to chlorophyll biosynthesis. Eur. J. Biochem. **225**, 529–537.

Pulido, P., Spinola, M.C., Kirchsteiger, K., Guinea, M., Pascual, M.B., Sahrawy, M., Sandalio, L.M., Dietz, K.J., Gonzalez, M., and Cejudo, F.J. (2010). Functional analysis of the pathways for 2-Cys peroxiredoxin reduction in *Arabidopsis thaliana* chloroplasts. J. Exp. Bot. **61**, 4043–4054.

Ramel, F., Birtic, S., Ginies, C., Soubigou-Taconnat, L., Triantaphylides, C., and Havaux, M. (2012). Carotenoid oxidation products are stress signals that mediate gene responses to singlet oxygen in plants. Proc. Natl Acad. Sci. U S A. **109**, 5535–5540.

Richter, A.S., Peter, E., Rothbart, M., Schlicke, H., Toivola, J., Rintamaki, E., and Grimm, B. (2013). Posttranslational influence of NADPH-dependent thioredoxin reductase C on enzymes in tetrapyrrole synthesis. Plant Physiol. **162**, 63–73.

Rizhsky, L., Davletova, S., Liang, H., and Mittler, R. (2004). The zinc finger protein Zat12 is required for cytosolic ascorbate peroxidase 1 expression during oxidative stress in *Arabidopsis*. J. Biol. Chem. **279**, 11736–11743.

Rodermel, S. (2001). Pathways of plastid-to-nucleus signaling. Trends Plant Sci. **6**, 471–478.

Ruckle, M.E., DeMarco, S.M., and Larkin, R.M. (2007). Plastid signals remodel light signaling networks and are essential for efficient chloroplast biogenesis in *Arabidopsis*. Plant Cell. **19**, 3944–3960.

Scharfenberg, M., Mittermayr, L., von Roepenack-Lahaye, E., Schlicke, H., Grimm, B., Leister, D., and Kleine, T. (2013). Functional characterization of the two ferrochelatases in *Arabidopsis thaliana*. Plant Cell Environ. doi:10.1111/pce.12248.

Smyth, G.K. (2004). Linear models and empirical bayes methods for assessing differential expression in microarray experiments. Statistical Applications in Genetics and Molecular Biology. **3**, Article3.

Srivastava, A., Lake, V., Nogaj, L.A., Mayer, S.M., Willows, R.D., and Beale, S.I. (2005). The *Chlamydomonas reinhardtii* gtr gene encoding the tetrapyrrole biosynthetic enzyme glutamyl-tRNA reductase: structure of the gene and properties of the expressed enzyme. Plant Mol. Biol. **58**, 643–658.

Strand, A., Asami, T., Alonso, J., Ecker, J.R., and Chory, J. (2003). Chloroplast to nucleus communication triggered by accumulation of Mg-protoporphyrin IX. Nature. **421**, 79–83.

Susek, R.E., Ausubel, F.M., and Chory, J. (1993). Signal transduction mutants of *Arabidopsis* uncouple nuclear CAB and RBCS gene expression from chloroplast development. Cell. **74**, 787–799.

Terry, M.J., and Smith, A.G. (2013). A model for tetrapyrrole synthesis as the primary mechanism for plastid-to-nucleus signaling during chloroplast biogenesis. Frontiers in Plant Science. **4**, 14.

Voigt, C., Oster, U., Bornke, F., Jahns, P., Dietz, K.J., Leister, D., and Kleine, T. (2010). In-depth analysis of the distinctive effects of norflurazon implies that tetrapyrrole biosynthesis, organellar gene expression and ABA cooperate in the GUN-type of plastid signalling. Physiol. Plant. **138**, 503–519.

von Gromoff, E.D., Alawady, A., Meinecke, L., Grimm, B., and Beck, C.F. (2008). Heme, a plastid-derived regulator of nuclear gene expression in Chlamydomonas. Plant Cell. **20**, 552–567.

Wielopolska, A., Townley, H., Moore, I., Waterhouse, P., and Helliwell, C. (2005). A high-throughput inducible RNAi vector for plants. Plant Biotechnol. J. **3**, 583–590.

Woodson, J.D., and Chory, J. (2012). Organelle signaling: how stressed chloroplasts communicate with the nucleus. Curr. Biol. **22**, R690–R692.

Woodson, J.D., Perez-Ruiz, J.M., and Chory, J. (2011). Heme synthesis by plastid ferrochelatase I regulates nuclear gene expression in plants. Curr. Biol. **21**, 897–903.

Xiao, Y., Savchenko, T., Baidoo, E.E., Chehab, W.E., Hayden, D.M., Tolstikov, V., Corwin, J.A., Kliebenstein, D.J., Keasling, J.D., and Dehesh, K. (2012). Retrograde signaling by the plastidial metabolite MEcPP regulates expression of nuclear stress-response genes. Cell. **149**, 1525–1535.